Proc. Natl. Acad. Sci. USA
Vol. 95, pp. 8975–8980, July 1998
Neurobiology

Geometric and viscous components of the tortuosity of the extracellular space in the brain

(diffusion/volume transmission/viscosity/extrasynaptic signaling/spillover)

DMITRI A. RUSAKOV* AND DIMITRI M. KULLMANN†‡

*Division of Neurophysiology, National Institute for Medical Research, The Ridgeway, Mill Hill, London NW7 1AA, United Kingdom; and †University Department of Clinical Neurology, Institute of Neurology, Queen Square, London WC1N 3BG, United Kingdom

Edited by Charles F. Stevens, The Salk Institute for Biological Studies, La Jolla, CA, and approved May 18, 1998 (received for review April 10, 1998)

ABSTRACT **To understand the function of neuro-active molecules, it is necessary to know how far they can diffuse in the brain. Experimental measurements show that substances confined to the extracellular space diffuse more slowly than in free solution. The diffusion coefficients in the two situations are commonly related by a tortuosity factor, which represents the increase in path length in a porous medium approximating the brain tissue. Thus far, it has not been clear what component of tortuosity is due to cellular obstacles and what component represents interactions with the extracellular medium ("geometric" and "viscous" tortuosity, respectively). We show that the geometric tortuosity of any random assembly of space-filling obstacles has a unique value (≈1.40 for radial flux and ≈1.57 for linear flux) irrespective of their size and shape, as long as their surfaces have no preferred orientation. We also argue that the Stokes–Einstein law is likely to be violated in the extracellular medium. For molecules whose size is comparable with the extracellular cleft, the predominant effect is the viscous drag of the cell walls. For small diffusing particles, in contrast, macromolecular obstacles in the extracellular space retard diffusion. The main parameters relating the diffusion coefficient within the extracellular medium to that in free solution are the intercellular gap width and the volume fraction occupied by macromolecules. The upper limit of tortuosity for small molecules predicted by this theory is ≈2.2 (implying a diffusion coefficient approximately five times lower than that in a free medium). The results provide a quantitative framework to estimate the diffusion of molecules ranging in size from Ca^{2+} ions to neurotrophins.**

Signaling between neurons in the brain takes place principally via the passive movement of substances in the extracellular space. A quantitative description of extracellular diffusion is therefore of central importance to understand both conventional "fast" amino acid neurotransmission, and more diffuse forms of chemical transmission as exemplified by monoaminergic and peptidergic signaling (1, 2, 3). The distinction between these modes of intercellular communication is in fact blurred by reports that the fast transmitters glutamate and γ-aminobutyric acid also may act at receptors outside the synaptic cleft where they are released (4, 5, 6, 7, 8).

The role of extracellular diffusion is not confined to chemical transmission: if extracellular diffusion of Ca^{2+} ions is slow, they may become locally depleted in the vicinity of foci of neuronal activity, thereby modifying synaptic efficacy (9, 10). All of the above phenomena also are linked intimately with pathological processes: changes in extracellular diffusivity have been described in the very early stages of cerebral ischemia, both with diffusion-weighted magnetic resonance imaging (11, 12) and with electrochemical measurements of inorganic ions injected into the extracellular space (13, 14, 15). These changes, which are likely to play a major role in neurotoxicity and seizure initiation, again underline the need for a comprehensive description of extracellular diffusion.

In spite of the fundamental role of extracellular diffusion, its properties are incompletely understood. Nicholson and colleagues (16) made an important advance by introducing a robust approximation approach, which considers diffusion in brain tissue as occurring within a porous medium. Assuming that cell membranes are relatively impermeable, Fick's laws of diffusion apply to such a medium, provided that two additional parameters are accounted for: the extracellular volume fraction α and the tortuosity λ (17). The latter parameter represents the "porous-to-free" increase in the path length of diffusing particles, which lowers the apparent diffusion coefficient by a factor $1/\lambda^2$.

The values of α and λ have hitherto been estimated in various brain areas by comparing the concentration profiles of dyes or inorganic ions injected into the brain with the corresponding solutions of diffusion equations (16, 18, 19, 20). Simultaneous measurements of α and λ also have been reported in the same tissue in the face of alterations in osmolarity, either by direct manipulation of the perfusion medium *in vitro* (21) or secondary to ischemia *in vivo* (13, 15). These experiments show that changes in α and λ are anticorrelated, although a quantitative explanation of this relationship is lacking. It is also unclear which component of the measured tortuosity arises from the tissue geometry alone (a component termed "geometric tortuosity" in this study), and which is due to nonelastic interaction of the diffusing molecules with cell walls and extracellular macromolecules (the "viscosity component" of tortuosity). This knowledge is however of critical importance, both to relate diffusion to tissue morphology and to gain a fuller understanding of the phenomena that determine the movement of molecules between cells.

We have demonstrated recently that the geometric tortuosity of the neuropil can be estimated by applying principles of integral geometry (22). Here, we show that the geometric tortuosity has a unique value if the tissue area of interest is homogeneous and isotropic. We further show that two important principles together determine the viscosity component of tortuosity. For small diffusing molecules, extracellular macromolecules can be considered as obstacles, which impose an additional increase in path length, analogous to the geometric obstacles formed by cells themselves. For larger diffusing molecules, comparable in size to the intercellular gaps, the rate of movement down the concentration gradient is further reduced, mainly because of viscous interactions with cell walls.

The publication costs of this article were defrayed in part by page charge payment. This article must therefore be hereby marked "*advertisement*" in accordance with 18 U.S.C. §1734 solely to indicate this fact.

This paper was submitted directly (Track II) to the *Proceedings* office.

‡To whom reprint requests should be addressed. e-mail: dkullman@ion.ucl.ac.uk.

We demonstrate consistency between the predictions derived from this treatment of viscosity and published experimental data, implying that it can be applied to derive quantitative predictions of the spatio-temporal extent of movement of molecules in the brain.

RESULTS

Infinitesimal Approximation. The porous medium approximation (16) implies that the extracellular space in brain tissue represents a continuous system of narrow, interconnected intercellular gaps (roughly equivalent to the soap phase in soap foam), as depicted schematically in Fig. 1*A*. First, we shall estimate the geometric tortuosity of such a medium, that is the porous-to-free path length increase of diffusing particles. We shall analyze the path of these particles within the extracellular space by considering the elementary path segments within a thin (thickness *dx*) and narrow (width *dy*) rectangular prism "probe" normal to *OX*, the direction of the general diffusion gradient (Fig. 1*A*). If the intercellular gaps are much smaller than the obstacles to diffusion, this probe cuts out a thin extracellular space fragment approximated by a parallelogram *K* as shown in Fig. 1*B*. The angular position of *K* in Euclidian space is determined by a pair of angles, β_1 and β_2 (see Fig. 1*B*). The flowing particles cross the slab along an "optimal" path $PQ = dq$ that lies on *K*, whereas in a free medium the particles would be simply translated along the segment *dx*. The direction of path *dq* is determined by the vector ***N*** normal to the surface *K* and the concentration gradient "driving force" ***f*** parallel to *OX*, which acts upon the particles (from thermodynamic principles,

$$f = \frac{1}{N_A}\frac{\partial \mu_i}{\partial x},$$

where $N_A = 6.02 \times 10^{23}$ mol^{-1} is Avogadro's number and μ_i is the partial molal Gibbs free energy, a quantity proportional to concentration). Two other forces act on the particles but do not affect the direction of *dq*: a Brownian stochastic force, whose time-and-space average equals zero, and friction or viscosity, which is antiparallel to the particle velocity vector. Thus, the direction of the path *dq* is defined by the intercept of *K* and a plane containing ***N*** and ***f*** (see Fig. 1*B*). Geometric principles give the relationship:

$$dq/dx = (1 + \cos^2\beta_1 \cdot \tan^2\beta_2)^{1/2}. \qquad \textbf{[1]}$$

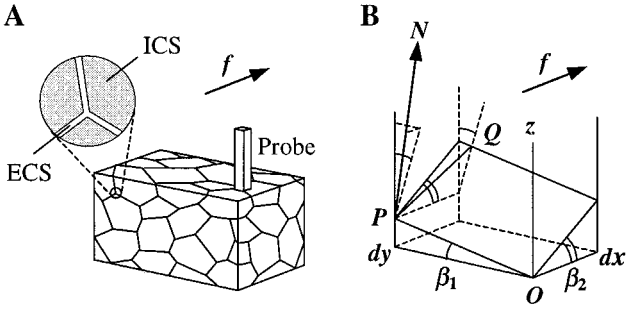

FIG. 1. Diagram illustrating derivation of the elementary geometric tortuosity of a porous medium. (*A*) A schematic diagram of a porous medium fragment with a thin and narrow rectangular prism probe situated perpendicular to the direction of diffusion ***f***. The expanded section shows the relationship of extracellular and intracellular spaces (ECS and ICS, respectively). (*B*) Geometry of the infinitesimal approximation: the thin and narrow probe cuts a parallelogram *K* out of the extracellular space (between two cell surfaces); a diffusing particle encounters the probe at point P and then travels on surface *K* along path $dq = PQ$; the spatial position of *K* is determined by angles β_1 and β_2 (shown).

Because *dq* is the particle path in the porous medium and *dx* would be the particle path in a free medium, the ratio *dq*/*dx* represents the "elementary geometric tortuosity". Eq. **1** provides an elementary basis to estimate the mean tortuosity factor that retards diffusion throughout the entire medium. This factor is slightly different, depending on whether it is calculated with respect to unidirectional or radial diffusion flow, as shown below.

Mean Geometric Tortuosity: Unidirectional Flux. We shall begin by considering unidirectional flux (ref. 23, pp. 273–281) in which the net movement of diffusing particles is in the direction *OX* and the average flux in directions *OY* or *OZ* equals zero (Fig. 1*A*). In physiological terms, this scenario occurs, for instance, when the diffusion source or sink is a planar surface of brain tissue. It also applies to the movement of water molecules that is detected by diffusion-weighted magnetic resonance imaging. The infinitesimal approximation illustrated in Fig. 1*B* allows estimation of the mean tortuosity λ_x by averaging the elementary geometric tortuosity across many thin slabs normal to the axis *OX*, the direction of diffusion. In other words, λ_x is determined by the mean $\langle dq/dx \rangle$ with respect to the complete set of parallel thin slabs, of which one is depicted in Fig. 1*B*. Therefore, to estimate λ_x from Eq. **1**, it is sufficient to determine the joint probability density of β_1 and β_2 in such a set (the joint probability density is required because orthogonal sections of arbitrary surfaces may not be statistically independent, ref. 24). Also note that in conditions of steady-state diffusion, this derivation is independent of surface concavity.

If the medium is isotropic (see *Discussion* for the case of an anisotropic medium), the vectors ***N*** normal to the elementary cell surface fragments (Fig. 1*B*) must point in any direction in space with equal probability. In other words, if we relate the occurrence of each such direction to the length of the corresponding vector ***N***, the vector vertices will form the sphere illustrated in Fig. 2*A*. This sphere, defined by $x^2 + y^2 + z^2 = r^2$ (where *r* is the arbitrary radius), thus represents the probability density function of the orientation of elementary cell surface fragments such as *K*. Therefore, sampling of fragments *K* in an isotropic medium is equivalent to the sampling of *K* on the spherical surface illustrated in Fig. 2*A*. The Euclidean coordinates (x, y, z) and angles β_1 and β_2 (see Fig. 2*A*) for each fragment *K*, resulting from the intersection of a thin slab and the sphere, are related as

$$\cos\beta_1 = z \cdot (y^2 + z^2)^{-1/2} \qquad \textbf{[2a]}$$

$$\tan\beta_2 = x/z. \qquad \textbf{[2b]}$$

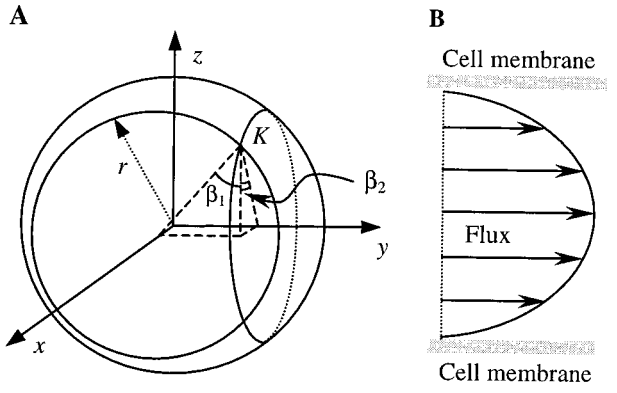

FIG. 2. (*A*) Sphere representing the probability density function of the directions of the vectors *N* (see Fig. 1*B*) normal to the elementary surface fragments *K*, in the case of an isotropic medium. The position of a fragment *K* sampled on the sphere is determined by angles β_1 and β_2. (*B*) Theoretical profile of the velocity of particles flowing between parallel cell walls. The profile corresponds to Eqs. **7–9** and applies for large diffusing molecules.

Combining Eqs. **1** and **2** gives

$$dq/dx = (1\text{-}x^2/r^2)^{-1/2}. \quad \textbf{[3]}$$

Eq. **3** allows, after a few elementary transformations, the averaging integral for λ_x over all slabs normal to *OX* (Fig. 1*B*) in the form

$$\lambda_x = \int_0^r \frac{dx}{\sqrt{r^2 - x^2}}. \quad \textbf{[4]}$$

This integral is convergent and yields $\lambda_x = \pi/2 \cong 1.571$, which therefore estimates the mean geometric tortuosity in the case of unidirectional diffusion flow through an isotropic medium.

Mean Geometric Tortuosity: Radial Flux. Radial diffusion is more commonly encountered in considering intercellular signaling and arises, for instance, when a vesicle of neurotransmitter is released within a small volume of tissue. In contrast to unidirectional diffusion, the mean tortuosity λ_r with respect to radial diffusion can be estimated by averaging the elementary geometric tortuosity over the complete set of thin slabs (see Fig. 1*A*) sampled in all possible directions with uniform probability. This estimate can be achieved as follows. First, Eq. **3** is transformed into spherical coordinates

$$dq/dr = (1\text{-}\sin^2\theta\cdot\cos^2\varphi)^{-1/2}. \quad \textbf{[5]}$$

And second, this expression is averaged over angles $0 < \theta < \pi$ and $0 < \varphi < 2\pi$, using a Monte Carlo experiment where θ and φ are distributed uniformly over their domains. This simulation experiment (sample size $n = 10{,}000$) gave the mean tortuosity for radial diffusion: $\lambda_r \cong 1.398$.

Nongeometric Component of Tortuosity: Viscosity. In a viscous medium, the fundamental Stokes–Einstein law relates the diffusion coefficient D to the effective radius of the diffusing molecules R, and the viscosity of the medium η:

$$D = \frac{kT}{6\pi\eta R}, \quad \textbf{[6a]}$$

where T is temperature and $k = 1.38 \times 10^{-23}$ J/K is Boltzmann's constant. If the aqueous medium also contains large particles, its viscosity η is given by

$$\frac{\eta}{\eta_0} = 1 + 2.5\phi + f(\phi), \quad \textbf{[6b]}$$

where ϕ is the volume fraction occupied by the large particles, η_0 is the viscosity of the aqueous phase (without these particles), and $f(\phi)$ is a term which represents deviations of the law to particular nonideal systems. However, relationships **6a** and **6b** cannot be applied generally to the extracellular medium because they require two conditions to be met. First, the diffusing molecules must be much smaller than the medium dimensions (intercellular gap width), so that their interaction with the stationary cell walls is negligible. This condition may be met for small ion species and most neurotransmitters whose effective dimensions in the aqueous solution are smaller than $\approx$1 nm. The situation is different for larger molecules such as neurotrophins and other polypeptides. In this case, according to the classic theory of viscosity, the predominant phenomenon is likely to be stationary wall drag. Wall drag affects the flux velocity v at different distances z from the stationary surface according to a fundamental formula

$$\frac{dv}{dz} = \frac{v}{R} \quad \textbf{[7]}$$

(where the hydrodynamic radius R also stands for the width of an elementary layer in the flux). If molecules flow between two approximately parallel surfaces (cell walls) spaced at a distance d apart, the boundary conditions for Eq. **7** are: $v(0) = v(d) = 0$ and $v(z \to \infty, d \to \infty) = V_{free}$, where V_{free} is the flux velocity unconstrained by the wall drag (i.e., in a free medium). Integration leads to an expression

$$v = V_{free}(1 + e^{-\frac{d}{R}} - e^{-\frac{z}{R}} - e^{-\frac{d-z}{R}}), \quad \textbf{[8]}$$

which suggests that the profile of the flux velocity $v(z)$ between two parallel cell walls follows a superimposition of two exponents, as depicted in Fig. 2*B*. Averaging v over the intercellular gap width d by using Eq. **8** yields the mean velocity $\langle v \rangle$ of the molecules flowing between the walls

$$\frac{\langle v \rangle}{V_{free}} = 1 + e^{-\frac{d}{R}} - \frac{2R}{d}(1 - e^{-\frac{d}{R}}). \quad \textbf{[9]}$$

An important feature of Eq. **9** is that the ratio

$$\frac{\langle v \rangle}{V_{free}},$$

in accordance with Fick's 1st law, is equivalent to the ratio between the diffusion coefficient in the extracellular space and that in a free medium, D/D_{free}. Eq. **9** also indicates that the effect of the stationary wall drag becomes negligible whenever $R \ll d$: for instance, when $r = 0.05d$, $D = 0.9D_{free}$.

The second fundamental requirement for the Stokes–Einstein relationship **6** to hold is that the diffusing molecules must be much larger than the molecules that constitute the medium (25). This is likely to be violated in the extracellular space of the brain because it contains large macromolecules loosely attached to the cell walls. A more likely scenario is that, although the viscosity η of such a medium may increase rapidly with the volume fraction occupied by these large particles (in agreement with Einstein's law or its extended versions, as illustrated by Eq. **6b** (26), the diffusivity of relatively small molecules in the medium remains much less affected (27). The accurate liquid mechanics description of such systems is complicated because of the difficulty of treating "hydrodynamic tortuosity" (27) and accounting for the obstruction effect of large, slowly moving particles (25).

Bearing in mind the latter comment, we attempt an alternative approach. Classically, the viscous interactions between the diffusing particles and layers of the medium are treated while assuming a nonslip boundary condition (see Eq. **7**). Instead, we treat extracellular macromolecules (and the water molecules that they bind) as random obstacles that impose an additional path increase (28). We postulate that small diffusing molecules flow in the medium with a constant rate whereas the viscous drag phenomena in the vicinity of the macromolecules are simply reflected by the effective size (volume) of these obstacles. Denote an additional tortuosity factor arising in this system as λ^*. Because there is only one preferred direction of diffusion within each infinitesimal fragment of the extracellular space (see Fig. 1*B*), λ^* should be calculated with respect to unidirectional flux. Denote also as ϕ the tissue volume fraction of the extracellular obstacles to diffusion (macromolecules constituting the extracellular matrix). If these obstacles occupy almost the entire extracellular volume ($\phi = \alpha$), $\lambda^* = \lambda_x \cong 1.57$. When $\phi < \alpha$, a "typical" molecule encounters no obstacles within the extracellular space (that is, $\lambda^* \equiv 1$) for a ϕ/α portion of its path. The other $(1 - \phi/\alpha)$ portion of the path corresponds to a situation analogous that shown in Fig. 1*B*. Given the probabilistic nature of mean λ^*, the value of $\lambda^*(\phi)$ can then be estimated by using a Bayesian probability formula:

$$\lambda^*(\phi) = \lambda_x \times \frac{\phi}{\alpha} + \left(1 - \frac{\phi}{\alpha}\right) = 1 + 0.57 \times \frac{\phi}{\alpha}. \quad \textbf{[10]}$$

Dissecting Geometric and Nongeometric Tortuosity of the Extracellular Space. Given the technical difficulties of measuring the diffusivity of the extracellular medium, an obvious question arises: how valid (and useful) are the above theoretical considerations regarding extracellular diffusion in real brain tissue? To relate our derivations to existing experimental observations, let us assign all viscosity phenomena to a particle path increase factor λ^*, which is additional to the factor λ_r caused by the geometric tortuosity alone, that is, $\lambda = \lambda_r\lambda^*$. The apparent extracellular diffusion coefficient D_{ap} measured in brain tissue will therefore combine the effects of geometric tortuosity and viscosity, so that $D_{ap} = D_{free}(\lambda_r\lambda^*)^{-2}$. Depending on whether the diffusing molecules are relatively large or small, the main contribution to the value of λ^* will be determined by Eq. **9** or **10**, respectively.

Nicholson and Tao (29, 30) analyzed the diffusion of dextrans of different molecular weight in rat cortical slices by using an optical method. The data, showing a positive relation between λ and the estimated Stokes radii of the dextrans, R, are replotted in Fig. 3*A*. Assuming $d \cong 20$ nm (the average distance between adjacent cell membranes, as typically observed in electron micrographs of cortical neuropil), Eq. **9** yields the relationship shown by the dotted line. Given that there are no adjustable parameters in the theory, the agreement between the theoretical prediction and the data is surprisingly close.

Similarly, both Eqs. **9** and **10** predict that D_{ap} should be positively correlated with the extracellular volume fraction α (or mean intermembrane distance d), as long as there is no change in ϕ. A manipulation of α that satisfies this condition is redistribution of water between the intracellular and extracellular compartments, obtained either directly by manipulating the ionic composition (and thus osmolarity) of the perfusing medium or indirectly by inducing tissue ischemia. In this case, ϕ is the only free parameter, which can be estimated by fitting Eq. **10** to the available experimental observations on the diffusion of small molecules. Fig. 3*B* shows data from the rat cortex (13, 15) (combined data shown) and the turtle cerebellum (21), where λ was estimated by monitoring the extracellular diffusion of tetramethylammonium (TMA^+) ions. Eq. **10** provides a reasonable fit in both cases, giving values of $\phi \cong 0.07$ for the turtle cerebellum and $\phi \cong 0.04$ for the rat cortex (i.e., extracellular molecules effectively occupy a smaller fraction of the tissue volume in the rat cortex).

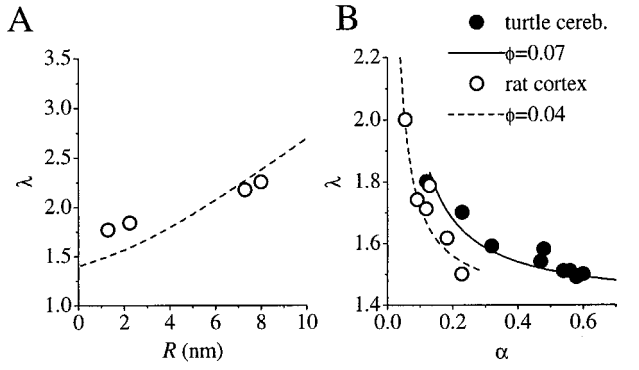

FIG. 3. (*A*) Comparison of theoretical estimates and experimental data relating the combined tortuosity λ to the effective radius of diffusing molecules. Circles, experimental estimates of the extracellular tortuosity in the rat cortex for four different dextrans (Stokes radii R are shown on the abscissa) by Tao and Nicholson (29, 30). Dashed line, theoretical prediction based on Eq. **9** with no adjustable parameters. (*B*) Comparison of theoretical estimates and experimental data relating the combined tortuosity λ to the extracellular volume fraction α. Filled circles, experimental estimates of α and λ measured with TMA^+ diffusion in the turtle cerebellum by Krizaj *et al.* (21), perfused with solutions of different osmolarities. Open circles, estimates of α and λ obtained in the rat neocortex by Pérez-Pinzón *et al.* (13) and Voříšek and Syková (15) in conditions of induced ischemia (combined data). Curves, corresponding theoretical estimates of $\lambda(\alpha)$, in accordance with Eq. **10** with one adjustable parameter, ϕ, the volume fraction occupied by large extracellular macromolecules.

Finally, our theory predicts that, for molecules much smaller than the intercellular gaps, the upper limit of the combined tortuosity λ is $\lambda_r\lambda_x \cong 2.2$ (see Eq. **10** when $\phi \to \alpha$). This value is not exceeded in any of the experimental measurements of TMA^+ diffusion (13, 15, 21, 31). Because the activation of glutamate receptors depends steeply on the effective diffusion coefficient (22), these results place constraints on the extent to which extrasynaptic receptors can be opened following exocytosis.

DISCUSSION

We have shown that the geometric tortuosity of an isotropic medium composed of space-filling obstacles has a unique value, ≈1.57 for unidirectional flux and 1.40 for radial flux. This result implies that, if the brain parenchyma is genuinely isotropic, deviations in λ from these values arise not from changes in tissue geometry but from the nongeometric, or viscosity, component of total tortuosity. Indeed, all the available estimates of λ, which is generally measured for radial flux, are in excess of 1.40, implying that the viscosity component is not negligible.

Tortuosity for Unidirectional and Radial Flux. Crank (23) and others have cautioned against extrapolating from detailed geometric treatments of unidirectional flux in heterogeneous media to other patterns of diffusion (ref. 23, p. 273). Nevertheless, a distinction between λ_x and λ_r, that is, between the tortuosity for unidirectional and radial flux, has not previously been made explicitly. The observation that the effective cumulative increase in path length caused by an arbitrary obstacle is generally greater for unidirectional than for radial flux can be illustrated by the following two-dimensional example. Consider a particle moving down a unidirectional concentration gradient (Fig. 4). In the absence of obstacles, it will cross successive iso-density contours, represented by parallel straight lines normal to the trajectory of the particle. However, when the particle's movement is restricted to a narrow "pore" (at an arbitrary angle θ with respect to the concentration

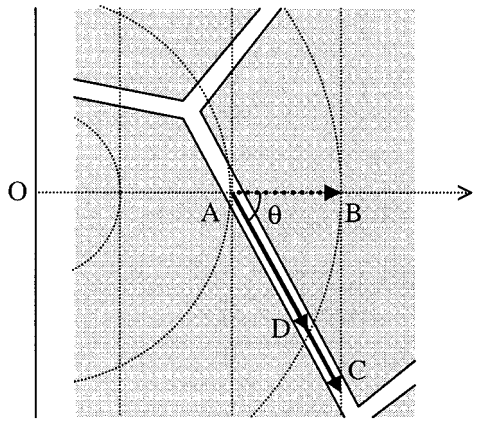

FIG. 4. Difference between tortuosity for unidirectional and radial flux. A particle at A, flowing down its concentration gradient (horizontal dotted arrow), is confined to an intercellular pore. In the case of unidirectional flux, it reaches the next iso-density contour (vertical dotted line) at C. In the absence of obstacles, it would have reached the next contour at B. The ratio of path length AC/AB, equivalent to $1/\cos\theta$, averaged over space, is thus equivalent to λ_x, the tortuosity for unidirectional flux. If, however, the diffusion flux is radial, originating from a point source at O, the particle only needs to travel as far as D to reach the next isodensity contour (circular dotted lines). The tortuosity for radial flux λ_r, is thus given by averaging the ratio AD/AB over space. Because AC > AD, it follows that $\lambda_x > \lambda_r$.

gradient), it will have to travel further than in a free medium (by a factor $1/\cos\theta$) to reach the next iso-density contour. In the case of radial diffusion, the iso-density contours are concentric circles, and the particle again travels further to reach the next contour, which is however always closer than for unidirectional flux (see Fig. 4). Because tortuosity is simply the average increase in path length for many such obstacles, it follows that λ_x (tortuosity for unidirectional flux) is greater than λ_r (tortuosity for radial flux).

Anisotropic Diffusion. A potential limitation on the present conclusions is the assumption that the brain is isotropic. Indeed, Nicholson, Syková and coworkers (15, 32, 33) have shown that the neuropil in some areas of the brain does exhibit minor degrees of anisotropy with respect to tortuosity. These measurements were obtained on a scale of 100 μm or more and do not necessarily preclude the occurrence of local isotropy at a smaller scale (for instance, intersynaptic distances). Nevertheless, it is important to establish whether the present analysis can be extended to the more general, anisotropic case. Although there is no general definition for an anisotropic medium, it can be conveniently introduced through the geometric formalism depicted in Fig. 2*A*. This can be used to relate the anisotropy of a medium with space-filling cells to a nonuniform spatial orientation of normal vectors ***N*** that determine the angular positions of elementary surface fragments. One natural example of such anisotropy is when the tissue can be considered as an initially isotropic medium stretched/compressed in one or two directions. In this case, the vertices of ***N*** form not a probability density sphere as depicted in Fig. 2*A*, but a three-axis ellipsoid. For an ellipsoid determined by $x^2/a^2 + y^2/b^2 + z^2/c^2 = 1$ (where a, b, and c are the three ellipsoid axes), the expression for local tortuosity, analogous to Eq. **3**, takes the form:

$$\frac{dq}{dx} = \sqrt{1 + \frac{b^4c^4x^2}{a^4(c^4y^2 + b^4z^2)}} \quad \text{where} \quad z^2 = c^2 - \frac{x^2}{a^2} - \frac{y^2}{b^2}. \quad \textbf{[11]}$$

Eq. **11** allows estimation of the mean tortuosity λ_x with respect to uni-directional diffusion along *OX* by using Monte Carlo averaging, where x and y are uniformly distributed within intervals $[0, a[$ and $[0, b[$, respectively. The estimated values of λ_x are shown in Table 1 for several characteristic ratios a:b:c. Note that the notion of "mean" tortuosity with respect to radial diffusion in this case is ambiguous because diffusion in an anisotropic medium occurs with different velocities in different directions.

A potential source of error in our approach is that estimates of λ from Eqs. **5** and **11** rely on Monte Carlo sampling experiments. This method was chosen because the explicit averaging integrals, although being finite by definition, showed unsatisfactory numerical convergence in the vicinity of singularities (data not shown). The numerical error that arises in our Monte Carlo simulations was assessed by the variation between the estimates obtained with different sample sizes, ranging from 5,000 to 15,000. This variation falls within $\pm$2–5% of the mean estimated value.

Table 1. Estimated values of the mean geometric tortuosity, λ_x, of a porous medium with different degrees of anisotropy of cell surfaces, characterized by the axes a, b, and c

Anisotropy axis ratio, a:b:c	Estimated tortuosity, λ_x
1:1:1*	1.56
1:1:2†	1.49
1:2:1†	1.39
1:2:2	1.76
2:1:1	1.09
2:2:1††	1.13
2:1:2††	1.17

*, Spherical surface: the Monte Carlo assessment is consistent with the analytical solution, giving $\lambda_x = \pi/2$ (see Results). Axis ratios marked with similar symbols († or ††) represent geometrically identical cases with respect to the direction of diffusion (differences in λ_x reflect the precision limit of the Monte Carlo simulations; see *Discussion*).

Mechanisms of Viscosity. We have argued that two different viscosity mechanisms contribute to the diffusion phenomena in the extracellular medium depending on whether the diffusing molecules are relatively large (Eq. **9**) or small (Eq. **10**). The distinction between these two mechanisms is, of course, somewhat artificial because molecules do not fall into two separate size classes. In addition, the diffusion of proteins with complex shapes and surface charge distributions may be affected by nonviscous interactions with extracellular receptors and other matrix molecules. The present derivations of the viscosity component of tortuosity should therefore be seen as the basis for further refinements. Nevertheless, the treatment of wall drag interactions with dextrans of different sizes does give a reasonable agreement with the data of Nicholson and Tao (29, 30) as depicted in Fig. 3*A*. Indeed, because the smaller dextrans encounter both viscosity mechanisms (wall drag and macromolecular obstacles), the discrepancy between the experimental fit and theoretical prediction may be even smaller than indicated.

We have argued that the retardation of extracellular diffusion due to viscosity is largely determined by the parameters ϕ, d, and α, rather than following the classic Stokes–Einstein theory. Although d and α can be estimated from electron micrographs (22), there does not appear to be a direct experimental approach to verify our predictions regarding ϕ, which represents the extracellular volume fraction occupied by large macromolecules (Fig. 3*B*). However, the prediction that the combined tortuosity λ is increased by extracellular macromolecules has been recently supported by experimental observations of Syková and coworkers (34): high molecular weight dextrans added to the perfusate caused large increases in λ, monitored in the isolated rat spinal cord by the diffusion of TMA^+. These results also can be used to compare the Stokes–Einstein theory (Eq. **6a**) and the Bayesian approximation (Eq. **10**). To test the applicability of the Stokes–Einstein law, we examined the effect of different dextran concentrations on the viscosity of the perfusate by using a falling ball viscometer (Gilmont, Barrington, IL). The results, related to the baseline value obtained for standard artificial cerebrospinal fluid (ACSF), were then used to derive an estimate of the relative diffusion coefficient (Eq. **6a**), and consequently apparent tortuosity λ in the presence of dextrans. For the Bayesian description (Eq. **10**), we referred to data from Tao and Nicholson (30): the hydrodynamic radii of both 40 kDa and 70 kDa dextran were reported to be $\approx$8 nm, implying that, in a 1% solution, the macromolecules occupy $\approx$20% of the volume. Under baseline conditions in the rat central nervous system, $\lambda \cong 1.57$ (ref. 34), implying $\phi/\alpha \cong 0.22$ (Fig. 3*B*). Eq. **10** can then be applied to predict the effect of adding specified concentrations of dextrans on ϕ and therefore λ. The outcome of the two alternative models is shown in Table 2, which indicates that the Stokes–Einstein description (Eq. **6a**) yields a larger deviation from the experimental data than the Bayesian description (Eq. **10**). This implies that the effect of large, slowly moving obstacles on the extracellular diffusion of small molecules, as described above, cannot be ignored.

An important aspect of the above considerations is that local narrowing of the intercellular gaps may significantly retard the diffusing flux in a supra-linear manner, whatever the size of the diffusing molecules. This phenomenon is reminiscent of the distinction between "local" and "global" viscosity observed in aqueous solutions containing large biological molecules (26, 27). It is therefore important to bear structural inhomogeneities in mind in considering diffusion on a small scale, for instance in the vicinity of a synapse.

Table 2. Comparison of experimental data and theoretical predictions for the effect of exogenous extracellular macromolecules (dextrans) on the tortuosity factor λ

Prefusate medium	Experimental data*	Bayesian approximation, (Eq. **10**)		Stokes–Einstein prediction, (Eq. **6**)	
	λ	ϕ/α	λ	η, mPas	λ
ACSF	1.57	0.22	(1.57)	1.05	(1.57)
+1% 70 kDa	1.75	0.38	1.70	1.47	1.85
+2% 70 kDa	1.72	0.54	1.83	1.70	2.00
+2% 40 kDa	1.77	0.54	1.83	1.47	1.85

*Data from Prokopová et al (34): Left column, artificial cerebrospinal fluid (ACSF) with various concentrations of 40 or 70 kDa dextran; ϕ/α, volume fraction of large molecules (including dextrans) in the extracellular space; η, viscosity of perfusate measured in mPas.

Apart from the geometric and viscous components of tortuosity, another phenomenon that affects the movement of neuroactive substances in the brain is the interaction of diffusing molecules with receptors, transporters and other binding sites. Although this interaction is beyond the scope of this paper, it can, under certain conditions, be treated as a buffering process that scales the diffusion coefficient in an analogous manner to tortuosity (22).

CONCLUSION

The present study separates tortuosity into two distinct components, geometric and viscosity. The finding that, for an isotropic porous medium, there is a unique value for geometric tortuosity is at first sight difficult to reconcile with the observation that osmotic perturbations, among other treatments, can have profound effects on the apparent diffusion path length. This paradox can however be fully explained by changes in viscosity arising from alterations in the distance between cell membranes and in the density of macromolecular obstacles. The approach outlined here allows a quantitative insight into the constraints on the movement of neuro-active substances in the extracellular medium and sheds light on the consequences of the early changes in extracellular space that accompany cerebral ischemia and other neuropathological states.

We are grateful to E. Syková for sharing unpublished data and to A. Fine and G. Barker for valuable comments on the manuscript. This work was supported by the Medical Research Council and the Biotechnology and Biological Sciences Research Council.

1. Agnati L. F., Zoli, M., Stromberg, I. & Fuxe, K. (1995) *Neuroscience* **69,** 711–726.
2. Zoli, M. & Agnati, L. F. (1996) *Prog. Neurobiol.* **49,** 363–380.
3. Bach-y-Rita, P. (1996) *Neuroscientist* **2,** 260–261.
4. Faber, D. S. & Korn, H. (1988) *Proc. Natl. Acad. Sci. USA* **85,** 8708–8712.
5. Isaacson, J. S., Solis, J. & Nicoll, R. A. (1993) *Neuron* **10,** 165–175.
6. Barbour B. & Häusser, M. (1997) *Trends Neurosci.* **20,** 377–384.
7. Kullmann, D. M. & Asztely, F. (1998) *Trends Neurosci.* **21,** 8–14.
8. Scanziani, M., Salin, P. A., Vogt, K. E., Malenka, R. C. & Nicoll, R. A. (1997) *Nature (London)* **385,** 630–634.
9. Montague, P. R. (1996) *Proc. Natl. Acad. Sci. USA* **93,** 3619–3623.
10. Rusakov, D. A., Harrison, E. & Stewart, M. G. (1998) *Neuropharmacol.* **37,** 513–521.
11. Mintorovich, J., Mosely, M. E., Chileuitt, L., Shimizu, H., Cohen, Y. & Weinstein, P. R. (1991) *Magn. Reson. Med.* **18,** 39–50.
12. Minematsu, K., Li, L., Fisher, M., Sotak, C. H., Davis, M. A. & Fiandaca, M. S. (1992) *Neurology* **42,** 235–240.
13. Pérez-Pinzón, M. A., Tao, L. & Nicholson, C. (1995) *J. Neurophysiol.* **74,** 565–573.
14. Syková, E. (1997) *Neuroscientist* **3,** 28–41.
15. Vořišek, I. & Syková, E. (1997) *J. Cereb. Blood Flow Metab.* **17,** 191–203.
16. Nicholson, C., Phillips, J. M. & Gardner-Medwin, A. R. (1979) *Brain Res.* **169,** 580–584.
17. Lehner, F. K. (1979) *Chem. Eng. Sci.* **34,** 821–825.
18. Nicholson, C. & Phillips, J. M. (1981) *J. Physiol.* **321,** 225–257.
19. McBain, C. J., Traynelis, S. F. & Dingledine, R. (1990) *Science* **249,** 674–677.
20. Nicholson, C. (1993) *J. Neurosci. Methods* **48,** 199–213.
21. Krizaj, D., Rice, M. E., Wardle, R. A. & Nicholson, C. (1996) *J. Physiol.* **492,** 887–896.
22. Rusakov, D. A. & Kullmann, D. M. (1998) *J. Neurosci.* **18,** 3158–3170.
23. Crank, J. (1975) *The Mathematics of Diffusion* (Clarendon, Oxford).
24. Rusakov, D. A. (1993) *Biometrics* **49,** 141–149.
25. Lamanna, R., Delmelle, M. & Cannistraro, S. (1994) *Phys. Rev. E Stat. Phys. Plasmas Fluids Relat. Interdiscip. Top.* **49,** 5878–5880.
26. Choy, T. C. (1995) *Physica A (Amsterdam)* **221,** 263–276.
27. Yam, K. L., Anderson, D. K. & Buxbaum, R. E. (1988) *Science* **241,** 330–332.
28. Clark, M. E., Burnell, E. E., Chapman, N. R. & Hinke, J. A. M. (1982) *Biophys. J.* **39,** 289–299.
29. Nicholson, C. & Tao, L. (1993) *Biophys. J.* **65,** 2277–2290.
30. Tao, L. & Nicholson, C. (1996) *Neuroscience* **75,** 839–847.
31. Van der Toorn, A., Syková, E., Dijkhuizen, R. M., Vořišek, I., Vargová, L., Škobisová, E., van Lookeren Campagne, M., Reese, T. & Nicolay, K. (1996) *Mag. Reson. Med.* **36,** 52–60.
32. Rice, M. E., Okada, Y. C. & Nicholson, C. (1993) *J. Neurophysiol.* **70,** 2035–2044.
33. Mazel, T., Šimonová, Z. & Syková, E. (1998) *NeuroReport* **9,** 1299–1304.
34. Prokopová, S., Nicholson, C. & Syková, E. (1996) *Physiol. Res.* **45,** 28.